STRATEGIES AND APPROACHES TO TPS DESIGN

Paul Kolodziej
NASA Ames Research Center
Moffett Field, CA, USA

ABSTRACT

Thermal protection systems (TPS) insulate planetary probes and Earth re-entry vehicles from the aerothermal heating experienced during hypersonic deceleration to the planet's surface. The systems are typically designed with some additional capability to compensate for both variations in the TPS material and for uncertainties in the heating environment. This additional capability, or robustness, also provides a "surge" capability for operating under abnormal severe conditions for a short period of time, and for unexpected events, such as meteoroid impact damage, that would detract from the nominal performance. Strategies and approaches to developing robust designs must also minimize mass because an extra kilogram of TPS displaces one kilogram of payload. Because aircraft structures must be optimized for minimum mass, reliability-based design approaches for mechanical components exist that minimize mass. Adapting these existing approaches to TPS component design takes advantage of the extensive work, knowledge, and experience from nearly fifty years of reliability-based design of mechanical components. A Non-Dimensional Load Interference (NDLI) method for calculating the thermal reliability of TPS components is presented in this lecture and applied to several examples. A sensitivity analysis from an existing numerical simulation of a carbon phenolic TPS provides insight into the effects of the various design parameters, and is used to demonstrate how sensitivity analysis may be used with NDLI to develop reliability-based designs of TPS components.

Paper presented at the RTO AVT Lecture Series on "Critical Technologies for Hypersonic Vehicle Development", held at the von Kármán Institute, Rhode-St-Genèse, Belgium, 10-14 May, 2004, and published in RTO-EN-AVT-116.

INTRODUCTION

The technology and engineering of Thermal Protection Systems (TPS) for hypersonic vehicles has significantly matured after nearly fifty years of development. The first modern TPS materials protected the military rockets of World War II from aerothermal heating during low Mach number flight. As time progressed, advanced materials were developed for more severe heating environments as vehicles flew at higher Mach numbers and for longer periods of time. Many strategies and approaches have been used over this period of time to design, test, and fabricate TPS. This lecture describes some of the successful strategies and approaches used in the past, and possibly those for the future.

Hypersonic vehicles are complex engineering designs that require the integration of many disciplines. With modern computer technology it is now possible to iterate on the vehicle geometry, aerodynamics, trajectory, structural design, and aerothermal/TPS design in a short period of time. These modern integrated design tools have eliminated much of the uncertainty in the calculation of aerothermal heating by performing a complete vehicle simulation along the entry trajectory, including angle of attack orientation. At very high velocities, several physical phenomena associated with the behavior of gases at high temperature, such as chemical dissociation, radiative heating, and boundary layer transition, become important. These modern tools have also significantly reduced the uncertainty in predicting aerothermal heating for many of these high temperature gas phenomena.

The thermal response of the TPS material to severe aerothermal heating is complicated, particularly when the material dissipates energy by ablation mechanisms, including sublimation and combustion. In many cases, experimental measurements of ablation in Arcjet ground facilities provide data essential for validating a numerical simulation of the material's thermal response that is used to predict behavior in flight. Because of differences between the ground test environment and the flight environment, TPS material performance in flight may be different than that predicted by the simulation.

The material properties used in these simulations are typically the values obtained from the manufacturer, and for some properties such as thermal conductivity, the value is dependent on temperature. The properties are typically the mean value of a measurement performed on several samples because small variations in the manufacturing process produce samples with slightly different properties. Measurement uncertainty that occurs when slightly different values are measured on the same sample also contributes to the distribution of values.

All of these uncertainties and variations affect the TPS design. Typically, the material thickness is increased to compensate for these effects in order to provide sufficient protection. Because this additional TPS mass directly subtracts from the payload mass, there is a strong incentive to use quantitative methods to assess the importance of the various effects and to specify the additional thickness required. Providing a reliable TPS design without a significant increase in mass is the goal of the following strategies and approaches.

TPS DESIGN STRATEGIES

Protecting the vehicle during all mission phases that have significant structural heating is the primary TPS objective. A secondary objective is to minimize changes in the surface geometry that affect the aerodynamics significantly enough to alter the vehicle orientation during flight.

Minimizing the TPS mass is important because one kilogram of TPS reduces the payload mass by one kilogram. On planetary missions that deploy an entry probe or lander reducing the TPS mass generally enables additional science perhaps in the form of another instrument, a larger power supply, or a more capable telemetry system. This mass penalty is even more severe on reusable launch vehicles where one kilogram of TPS reduces the payload delivery capability to low earth orbit by a kilogram for every mission.

One of the important strategies used in the development of early vehicle designs focused on maximizing the volumetric efficiency. Because TPS is attached to the exterior surface of the vehicle, geometries that enclose the largest volume with the smallest amount of surface area also minimize the area and mass of the TPS. Spheres are the most volumetrically efficient geometries, but have small aerodynamic capability for maneuvering to a landing site. Geometries that are aerodynamically shaped to provide hypersonic lift-to-drag ratios (L/D) that enable maneuvering during entry are less volumetrically efficient than a sphere. In general, the volumetric efficiency decreases with increasing L/D as shown in Fig. 1.[1] Selecting a vehicle geometry that maximizes the volumetric efficiency, and provides sufficient aerodynamic capability for maneuvering, is still an important TPS design strategy.

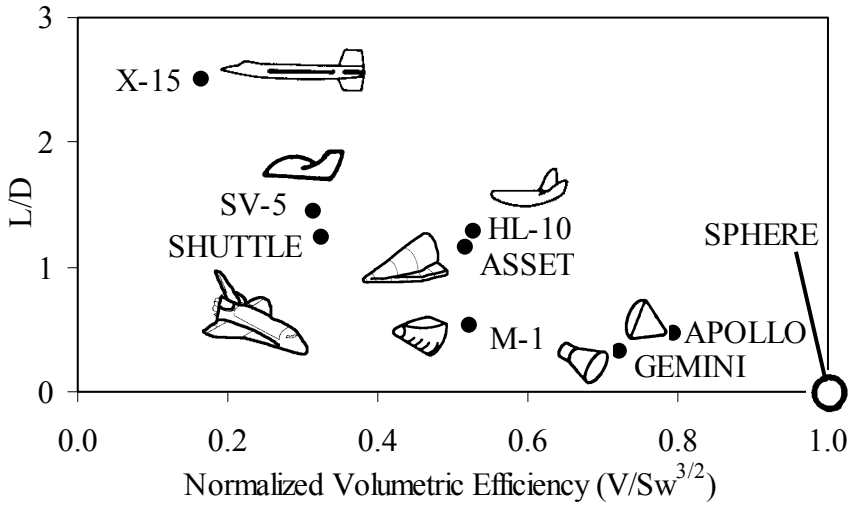

Figure 1: Volumetric efficiency decreases as the hypersonic lift-to-drag ratio increases.

The heating rates and temperatures of the TPS vary significantly at different locations on the vehicle. In general, the nose and leading edges of the wing and control surfaces experience the most severe heating and the highest temperatures. The leeward surfaces and the base region experience more moderate heating and operate at lower temperatures. As a historical

example, maximum temperatures measured on the hypersonic X-15 aircraft are shown in Fig. 2.[2]

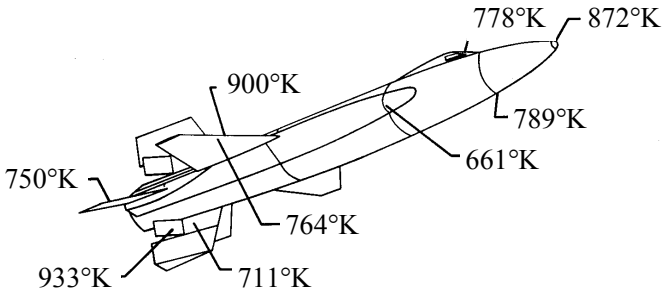

Figure 2: Maximum temperatures measured on the X-15 (Ref. 2).

Minimizing the area that is required to operate at very high temperatures, such as the wing leading edge, is another important design strategy that was recognized in the development of early vehicle concepts. In general, an area that experiences the most severe heating is protected with a high performance TPS, i.e. one able to operate at high temperatures or with a high total heat load capability. Areas that experience more moderate heating are usually protected with a TPS material that has a lower temperature or total heat load capability. The trends shown in Fig. 3 for early TPS materials indicate that TPS system weight increases with both heating rate (heat flux) and total heat load.[3] Similar trends are still valid today.

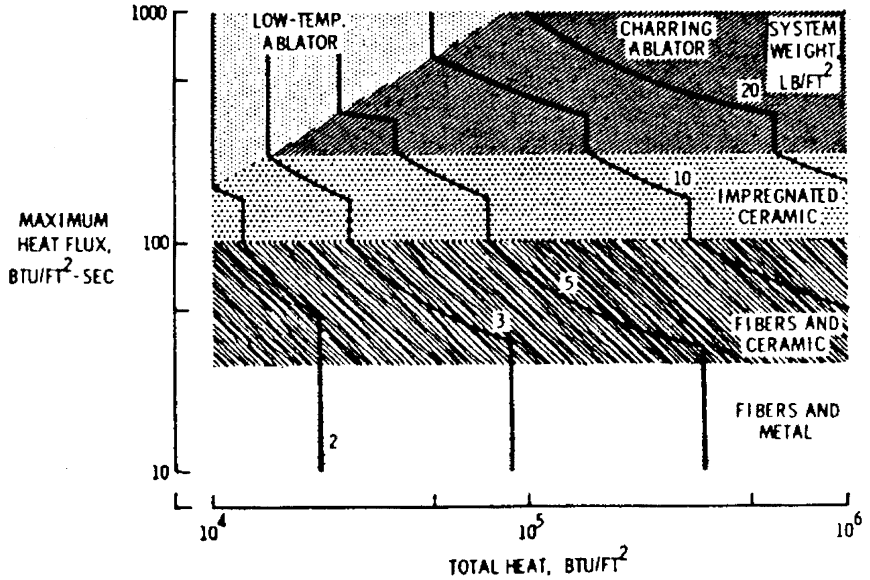

Figure 3: TPS system weight increases with maximum heat flux and total heat load (Ref. 3).

In addition to minimizing TPS mass, it is also important to design a robust system that tolerates unexpected events or conditions. Efforts to provide more protection and strengthen the design simply by increasing the TPS thickness, without quantitative criteria, often lead to a system with excess mass. A reliability-based approach to TPS design provides a

quantitative methodology for objective tradeoffs between materials, aerothermal heating loads, and robustness. This approach is a two-step process, where first the individual TPS components are designed for a specific reliability, and then the component reliabilities are summed into an overall system reliability by fault tree methods. This approach may be applied to the details of a TPS design including the joints, seals, ports, and access hatches necessary for assembly and installation on a vehicle. The following sections discuss an approach to calculating the thermal reliability of TPS components.

SENSITIVITY ANALYSIS

An important method used by many disciplines today is a sensitivity analysis, which provides insight into the effects of various parameters, and assists in identifying which parameters are most important. One of the best examples of a TPS sensitivity analysis examined the influence of thirty-nine parameters on the behavior of a carbon phenolic ablative thermal protection system.[4]

The nominal mission in Ref. 4 was a ballistic re-entry trajectory of an 8° half-angle cone with a ballistic coefficient of 14,660 Kg/m^2. Re-entry occurred at an altitude of 91.4 km with a velocity of 7,596 m/s at an entry angle of -19°. The steep ballistic trajectory caused a short duration, high convective heating environment. Maximum convective heating of 26.7 MJ/m^{2}s occurred at 32 seconds, and ground impact occurred at 40.7 seconds. The total convective heat load was 255 MJ/m^2.

First, a numerical simulation of the nominal mission was completed to size the carbon phenolic thickness at a location 30.5 cm behind the cone vertex. The carbon phenolic was attached to a 0.76 mm thick aluminum structure with a design temperature limit of 450°K. For nominal values of the thirty-nine parameters, a 9.8 mm thickness of carbon phenolic was required to limit the aluminum temperature to 450°K. Then, the effect of each parameter (P_i) was investigated by calculating the thickness required to limit the aluminum temperature to 450°K when one parameter at a time is perturbed, with the others held constant. The change in the carbon phenolic thickness indicated the sensitivity of the design to each parameter. Sensitivities to the properties of the aluminum structure and the initial temperature before entry were not analyzed.

The numerical simulation of ablation included important transport phenomena occurring at the surface and in the char, reaction zone, and virgin plastic. At the surface, convective heating was calculated for a turbulent boundary layer with equilibrium air properties. Decomposition of the virgin plastic employed a two-term Arrhenius rate law, and material properties varied with the amount of decomposition. All the material properties were from test data. The char thermal conductivity and specific heat alone were temperature dependent.

The results that follow show the effects of variability in the material property data and indicate which improvements in manufacturing may have the largest benefit. The results also show the effects of variability in the parameters controlling ablative thermal decomposition, and provide insight to enable the design of experimental programs that efficiently test the material and the numerical simulation model. Finally, the results are an important step in estimating the thermal reliability of the TPS design.

Virgin Plastic Properties

The effects of the virgin plastic properties on the carbon phenolic thickness, or gage (G), are shown in Fig. 4. The properties and thickness are normalized by their nominal values for direct comparison. Thermal conductivity (k_v), specific heat (Cp_v) and density (ρ_v) have the largest effect on the carbon phenolic thickness by influencing thermal diffusion. Increasing the heat of decomposition (H_D) increases the amount of heat absorbed by the decomposing material. Emissivity (ε_v) has a small effect because thermal radiation is negligible at the low temperatures of the virgin plastic. The reaction constants of the virgin plastic (A_v,B_v,n_v) have negligible effect. The specific heat alone exhibits nonlinear behavior.

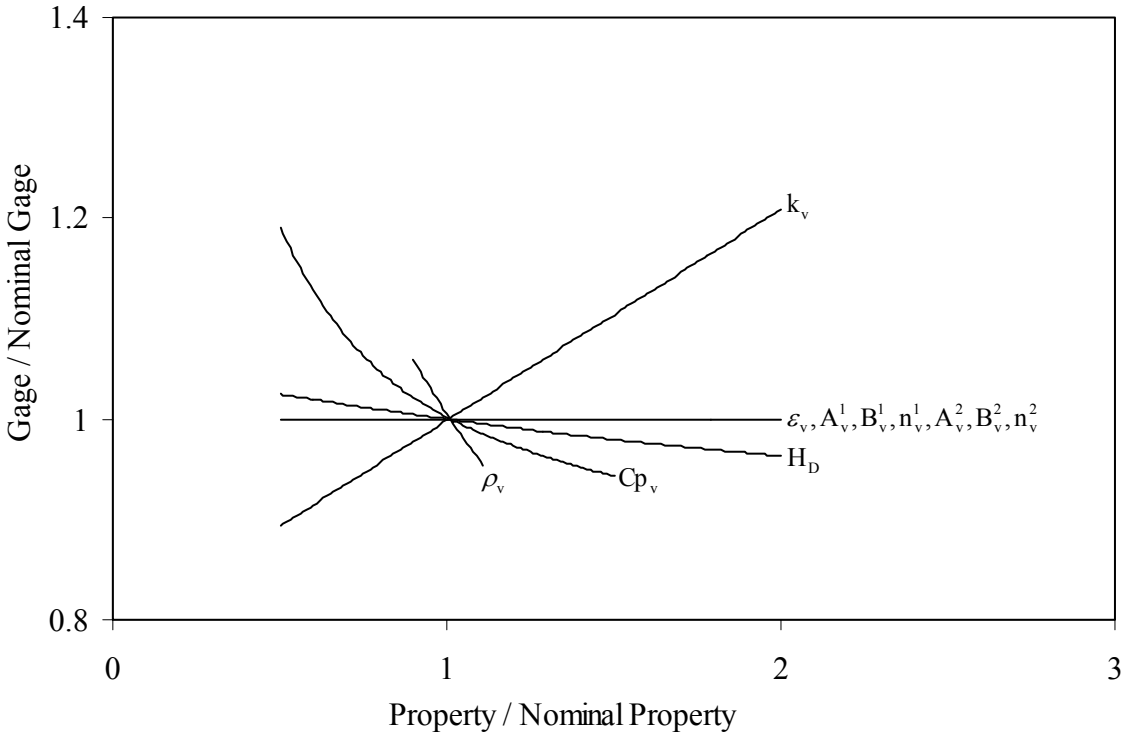

Figure 4: Virgin plastic properties (Ref. 4).

Many manufacturing processes produce materials with a statistical variation in physical properties. If the TPS design was fabricated with a carbon phenolic that has a higher thermal conductivity than the nominal value, the aluminum structure will exceed the design temperature limit (450 °K) unless the nominal thickness is increased. First derivatives ($\partial G/\partial P_i$) of the sensitivity curves in Fig. 4 demonstrate the relative importance of each parameter and indicate that of the virgin plastic properties the variability in density will have the largest effect on the carbon phenolic thickness.

Char Material Properties

The effects of the char material properties on the carbon phenolic thickness are shown in Fig. 5. Thermal conductivity (k_c) and specific heat (Cp_c) have a large effect on thickness by controlling thermal diffusion. The char density (ρ_c) has the largest nonlinear effect possibly

because it controls: thermal diffusion, the amount of material available for decomposition, and the decrease in material thickness. Emissivity (ε_c) has a large effect, because thermal radiation is significant at the high temperatures of the char.

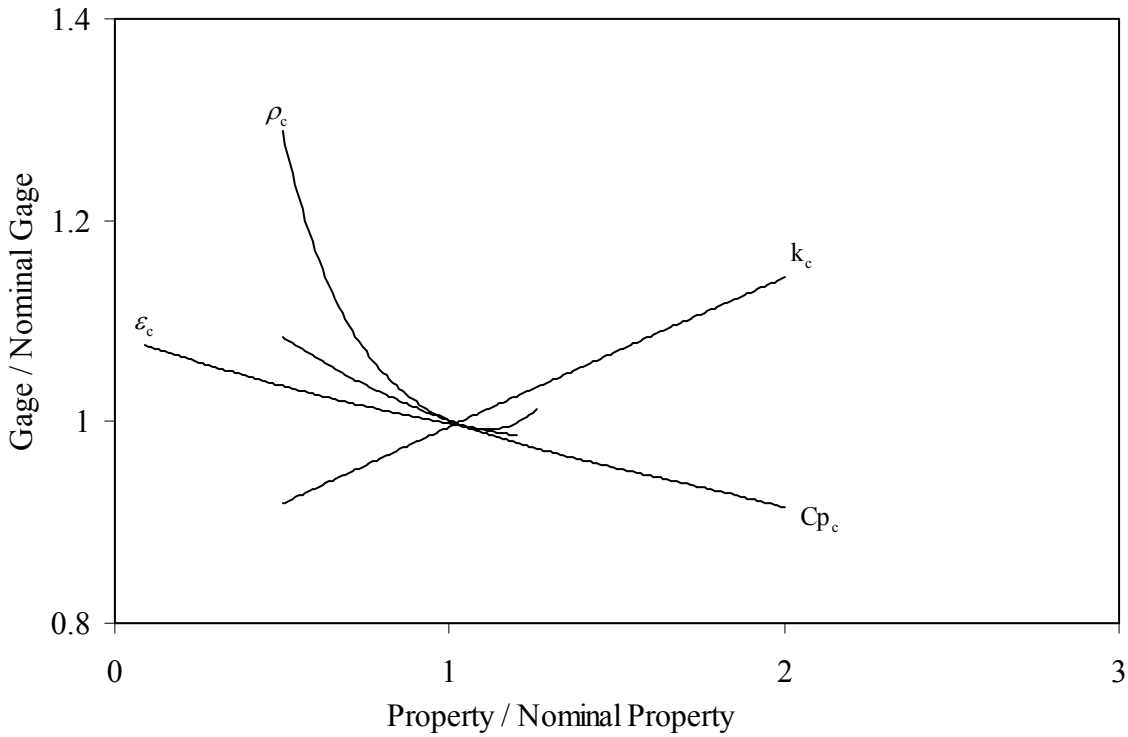

Figure 5: Char thermal properties (Ref. 4).

Char Recession Properties

The effects of the char recession properties on the carbon phenolic thickness are shown in Fig. 6. Because of the high surface temperatures, surface recession was in the diffusion combustion and sublimation regimes for carbon phenolic. Increasing the blowing parameter (B^*) directly increases surface recession and more material is required. Decreasing the activation temperature for sublimation (B_s) increases the sublimation of material at lower temperatures. The heat of sublimation (H_s) and the heat of combustion ($H_{c,c}$) have a smaller effect. The reaction constants of sublimation (A_s,B_s,n_s) and combustion (A_c,B_c,n_c) have negligible effect and are not shown.

Ablation Gas Properties

The effects of the ablation gas properties on the carbon phenolic thickness are shown in Fig. 7. Decreasing the transpiration factor (η_v) reduces the capability of the ablation gases to reduce the convective heat flux. Decreasing the transpiration factor for the char gases (η_c) has a similar effect. The specific heat (Cp_g) controls the storage of thermal energy in the gas as it diffuses through the char and has small effect. The heat of combustion ($H_{c,g}$) has a negligible

effect. In general, these properties have a smaller effect than the properties of the virgin plastic and char.

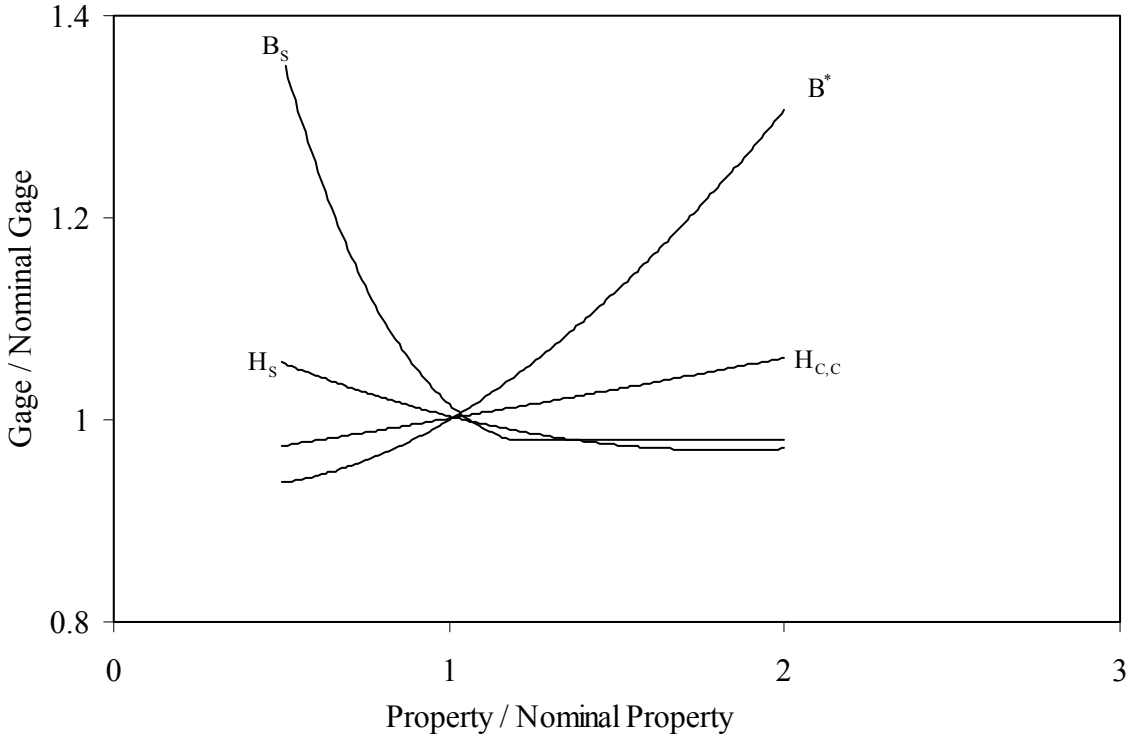

Figure 6: Char recession properties (Ref. 4).

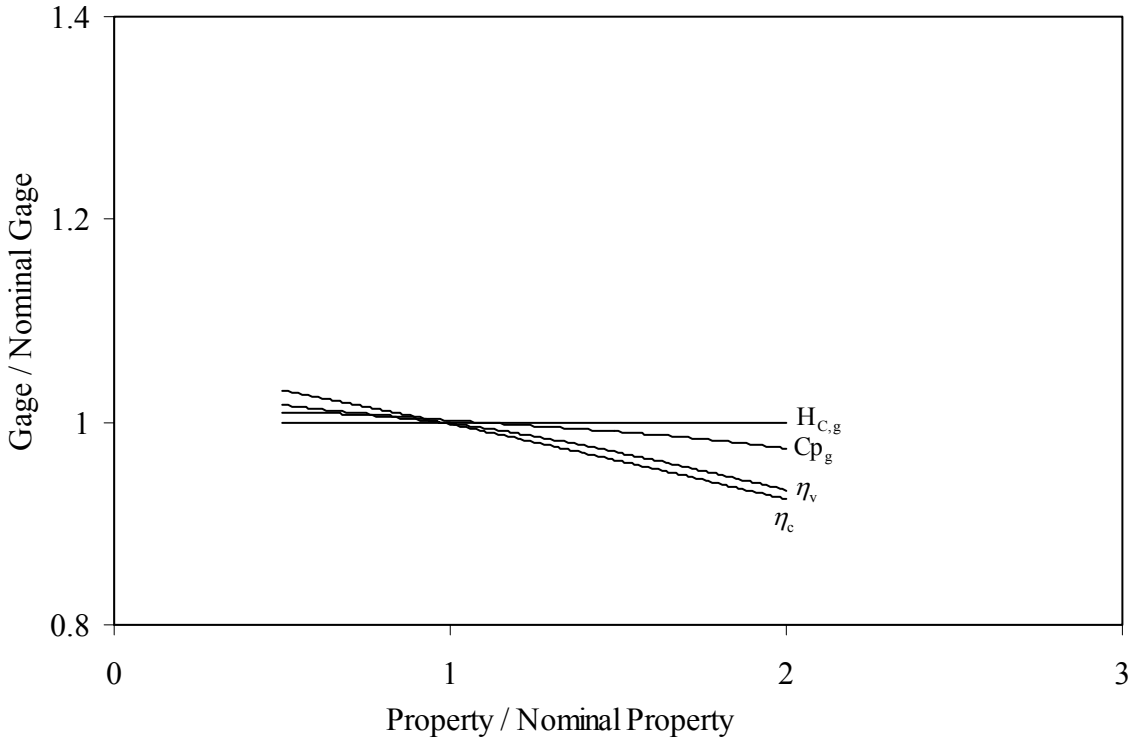

Figure 7: Ablation gas properties (Ref. 4).

Convective Heat Transfer

Because of the increasing Reynolds number during an entry trajectory the boundary layer will usually transition from laminar to turbulent flow. This transition may occur at higher altitudes than expected as the TPS begins to ablate and the boundary layer is destabilized by both gas and material that are injected into the flow. In some cases the surface may develop significant roughness that may also destabilize the boundary layer. Instead of attempting to predict when transition occurs, Ref. 4 used a conservative design approach that assumed a turbulent boundary layer for the entire trajectory. Turbulent heat transfer and shear rates at the surface are higher than those in laminar flow under comparable conditions. The effect of the heat transfer parameter (H) on carbon phenolic thickness is shown in Fig. 8.

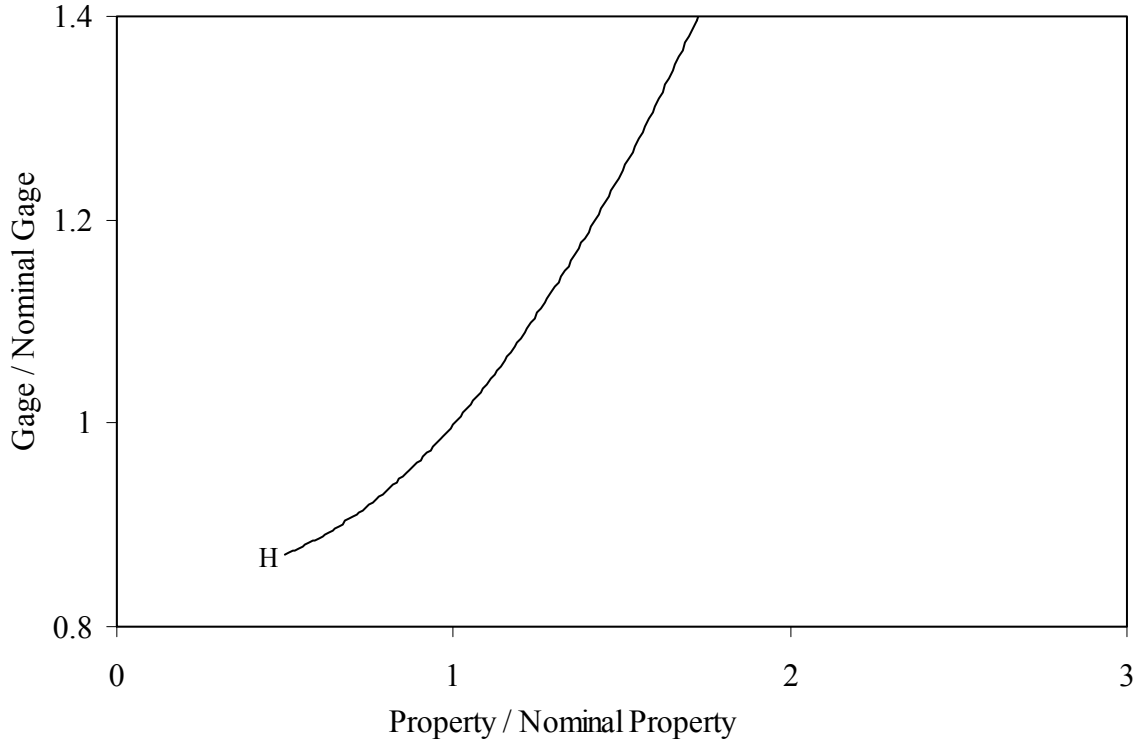

Figure 8: Heat transfer parameter (Ref. 4).

Sensitivity Analysis Summary

Table 1 lists the nine parameters that have largest effect ($|\partial G/\partial P_i| > 0.10$) on the carbon phenolic thickness. Three are properties of the virgin plastic and five are properties of the char layer. To establish confidence in using the numerical simulation as a design tool it is necessary to perform experiments that test the relationship between variation in each parameter and the thickness. Experiments that focus on the properties with the greatest $|\partial G/\partial P_i|$ provide the most benefit.

It is important to recognize that none of the nine parameters are defined by a single value, but are defined by a distribution of values. Several factors cause a distribution in values for each parameter including natural randomness, measurement uncertainty, and the statistical

distributions present in the manufacturing of many materials. Understanding the effect of these distributions on the TPS thickness provides additional insight into robust TPS design.

i	Property, P_i	$\partial G/\partial P_i$
1	Char Thermal Conductivity (k_c)	+0.995
2	Virgin Density (ρ_v)	-0.503
3	Heat Transfer Parameter (H)	+0.376
4	Sublimation Activation Temp. (B_s)	-0.292
5	Virgin Thermal Conductivity (k_v)	+0.210
6	Blowing Parameter (B^*)	+0.196
7	Virgin Specific Heat (Cp_v)	-0.172
8	Char Density (ρ_c)	-0.137
9	Char Specific Heat (Cp_c)	-0.121

Table 1: Sensitivity derivatives evaluated at nominal conditions.

In many cases, a normal (Gaussian) probability density function (PDF) may be used to describe the distribution of expected values for a parameter. For a normal distribution the PDF is specified by the mean (μ) value and standard deviation (σ), and more than 99.7 % of the distribution is found between the $\mu \pm 3\sigma$ limits. Each of the parameters in Table 1 may be represented by a non-dimensional PDF with a mean value equal to the nominal value. The 3σ limits are usually determined from the statistical analysis of: material property measurements, repetitive experimental measurements in ground facilities, and numerical analysis of the flight environment.

The Taylor series expansion in Eq. (1) may be used to analyze the effects of a PDF on the carbon phenolic thickness, and is accurate if the deviation of the parameters (Δ_i) is small and the parameters are statistically independent.

$$G = G_0 + \sum_{i=1}^{n} \left(\frac{\partial G}{\partial P_i} \right)_0 (\Delta_i)$$
$$\Delta_i = \left(P_i - P_{i,0} \right) \tag{1}$$

To minimize nonlinearities, it is important to select appropriate reference conditions ($P_{i,0}$), which, in this analysis are the nominal or mean values. Even when significant nonlinearities are present a Taylor series expansion provides valuable insight into the characteristics of the nominal design. The Taylor series is the basis for the extreme value (EV) and root-sum-square (RSS) methods that are commonly used to estimate the additional thickness, or margin, in TPS component design.

TPS MARGIN

Extreme Value Method

Increasing the carbon phenolic thickness provides margin to allow for variability in the parameters. The EV method in Eq. (2) provides a "worst case scenario" estimate of the

additional thickness (ΔG_E) required because all of the parameters are summed at their 3σ deviations ($\Delta_{i,3\sigma}$). The probability of this combination occurring is low, and adding ΔG_E to the nominal design is overly conservative. On the other hand, if only a 1σ deviation ($\Delta_{i,1\sigma}$) is used, there is a reasonable probability that a parameter will exceed $\Delta_{i,1\sigma}$ and cause a high temperature in the aluminum structure.

$$\Delta G_E = \sum_{i=1}^{n} \left| \left(\frac{\partial G}{\partial P_i} \right)_0 \left(\Delta_{i,3\sigma} \right) \right|$$
$$\Delta_{i,3\sigma} = P_{i,3\sigma} - P_{i,\mu} \qquad (2)$$
$$\Delta_{i,1\sigma} = P_{i,1\sigma} - P_{i,\mu}$$

Root-Sum-Square Method

If all of the parameters (P_i) are independent and the deviations ($\Delta_{i,3\sigma}$) are random, the additional thickness (ΔG_R) required is given by the root-sum-square in Eq. (3).

$$\Delta G_R = \sqrt{\sum_{i=1}^{n} \left(\left(\frac{\partial G}{\partial P_i} \right)_0 \left(\Delta_{i,3\sigma} \right) \right)^2} \qquad (3)$$

Again, by using $\Delta_{i,3\sigma}$ the additional thickness ΔG_R provides sufficient margin for 99.7% of the expected values of each P_i. Because $\Delta G_R \le \Delta G_E$, for the same values of $\partial G/\partial P_i$ and $\Delta_{i,3\sigma}$, the RSS method is less conservative than the EV method and has lower mass. A comparison between the two methods is shown in Table 2. To demonstrate these methods without disclosing information on material properties which in many cases may be proprietary, the 3σ deviations ($\Delta_{i,3\sigma}$) in Table 2 were assigned by a random number generator.

i	Property, P_i	$\partial G/\partial P_i$	$\Delta_{i,3\sigma}$	ΔG_i	$\lvert \Delta G_i \rvert$	$(\Delta G_i)^2$
1	Char Thermal Conductivity (k_c)	+0.995	0.426	+0.424	0.424	0.180
2	Virgin Density (ρ_v)	-0.503	0.979	-0.492	0.492	0.242
3	Heat Transfer Parameter (H)	+0.376	0.215	+0.081	0.081	0.007
4	Sublimation Activation Temp. (B_s)	-0.292	0.567	-0.165	0.165	0.027
5	Virgin Thermal Conductivity (k_v)	+0.210	0.943	+0.198	0.198	0.039
6	Blowing Parameter (B^*)	+0.196	0.571	+0.112	0.112	0.012
7	Virgin Specific Heat (Cp_v)	-0.172	0.523	-0.090	0.090	0.008
8	Char Density (ρ_c)	-0.137	0.305	-0.042	0.042	0.002
9	Char Specific Heat (Cp_c)	-0.121	0.821	-0.099	0.099	0.010

$\Delta G_E = \sum = 1.704$

$\Delta G_R = \sqrt{\sum} = 0.726$

Table 2: Comparison between the extreme value and root-sum-square methods.

ROBUST DESIGN OBJECTIVES

Modern components and devices are designed to operate reliably in environments with significant variation, under circumstances that are not well defined, and during unexpected random events. Several strategies used to provide this capability are:

1) Provide capability to degrade continuously in performance instead of failing catastrophically,
2) Provide short-term excess capacity or surge capability,
3) Provide fault tolerance for unexpected events,
4) Provide self-diagnostics and correction.

These strategies are also important goals for future TPS designs. The addition of margin, or a factor of safety to the TPS design, is an important approach to achieving these goals.

Mechanical component design and structural design are based on almost two-hundred years of experience, and the methods and approaches are much more mature than the methods used to design TPS components. It may be possible to significantly improve the methods and approaches to TPS design by adapting this experience, along with the relevant design guidelines, proven methods, and effective techniques. For example, Table 3 lists the factors of safety that are commonly used for different design environments and materials. Large factors of safety are used when there is high uncertainty or variation. Small factors of safety are used when the environment and materials are well defined.

FOS	Description
1.2 to 1.5	Exceptionally reliable materials used under controlled conditions
1.5 to 2	Well known materials used under reasonably constant environment conditions
2 to 2.5	Average materials operating in normal environments
2.5 to 3	Less tried or brittle materials under average conditions of loading
3 to 4	Untried materials used under average conditions, or better known materials used in uncertain environments
> 4	Untried materials used in uncertain environments

Table 3: Factors of Safety (FOS) that are commonly used for different design environments and materials.

In the past fifty years, mechanical designers have developed several methods to quantify the effect of a factor of safety on reliability. Many of these early quantitative methods were developed by the aircraft industry to design structures with minimum mass. Eliminating one kilogram of structure from an aircraft in the 1950s reduced the overall mass by as much as ten

kilograms. These methods used PDFs to describe the load environment and material strength, and developed quantitative estimates of the probability of failure (F), or reliability (1-F).

Strength-Load Interference Method

The strength-load interference method (see Fig. 9) is commonly used in the reliability-based design of mechanical components.[5]

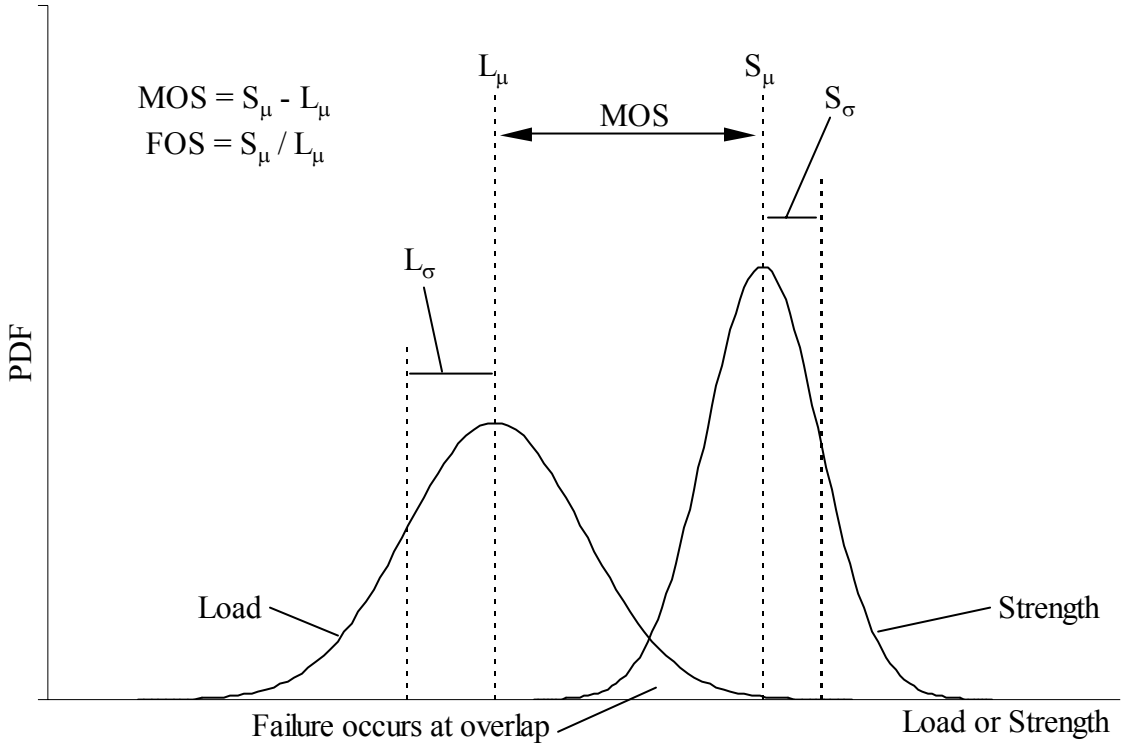

Figure 9: Strength-load interference of probability distribution functions.

For normal distributions of strength and load there are four key parameters required for estimating reliability:

1. Factor of safety (FOS) = S_μ / L_μ,
2. Margin of safety (MOS) = $S_\mu - L_\mu$,
3. Strength uncertainty ratio = S_σ / S_μ,
4. Load uncertainty ratio = L_σ / L_μ.

For normal probability distributions of strength and load, reliability is defined by:

$$R = \frac{1}{\sqrt{2\pi}} \int_{-\infty}^{IOR} \exp\left(\frac{-x^2}{2}\right) dx \qquad (5),$$

where the index of reliability (IOR) is given by

$$IOR = \frac{FOS - 1}{\sqrt{FOS^2 \left(\frac{S_\sigma}{S_\mu} \right)^2 + \left(\frac{L_\sigma}{L_\mu} \right)^2}} \qquad (6).$$

The factor of safety (FOS) is a ratio of the mean value of strength (S_μ) to the mean value of load (L_μ). Under extremely well defined conditions where S_σ and $L_\sigma = 0$, the strength and load are simply the mean values of the strength and load PDFs. If the design has a strength that equals the load ($S_\mu = L_\mu$) then FOS = 1, and there is a 50% probability of failure. Slightly increasing the load (FOS < 1) results in a 100% probability of failure, and if the strength is slightly increased (FOS > 1) there are no failures (100% reliability). Under less well defined conditions where S_σ and $L_\sigma > 0$, a 50% probability of failure still occurs if the PDFs describing strength and load are identical ($S_\mu = L_\mu$, $S_\sigma = L_\sigma$). Sufficiently increasing S_μ, such that all of the expected values of strength are greater than all of the expected values of load results in 100% reliability. The uncertainty ratio is also known as the coefficient of variation.

Reliability-based design is more complex when the strength PDF and load PDF overlap or interfere with each other, which frequently occurs when a design is optimized to minimize mass. Although numerical methods are typically used for the thermal-structural reliability analysis of sophisticated components, such as turbine blades, efficient design methods for preliminary estimates of thermal reliability alone are not readily available. An efficient method may be developed by adapting the strength-load interference method that is commonly used in the reliability-based design of mechanical components to the design of thermal components.

Intrinsic functions for evaluating the integral in Eq. (5) are available in commercial spreadsheet software. Fig. 10a-d shows some characteristic relationships between these parameters. In general, when FOS is small and L_σ / L_μ is large the reliability approaches 50%, and increasing the factor of safety increases the reliability. For a given L_σ / L_μ, the reliability decreases as S_σ / S_μ increases in Fig. 10a to 10d. Very high reliability at low FOS is achieved by minimizing L_σ / L_μ, first by conducting experiments and analysis to characterize the load environment, and then by developing techniques to minimize the variation in load.

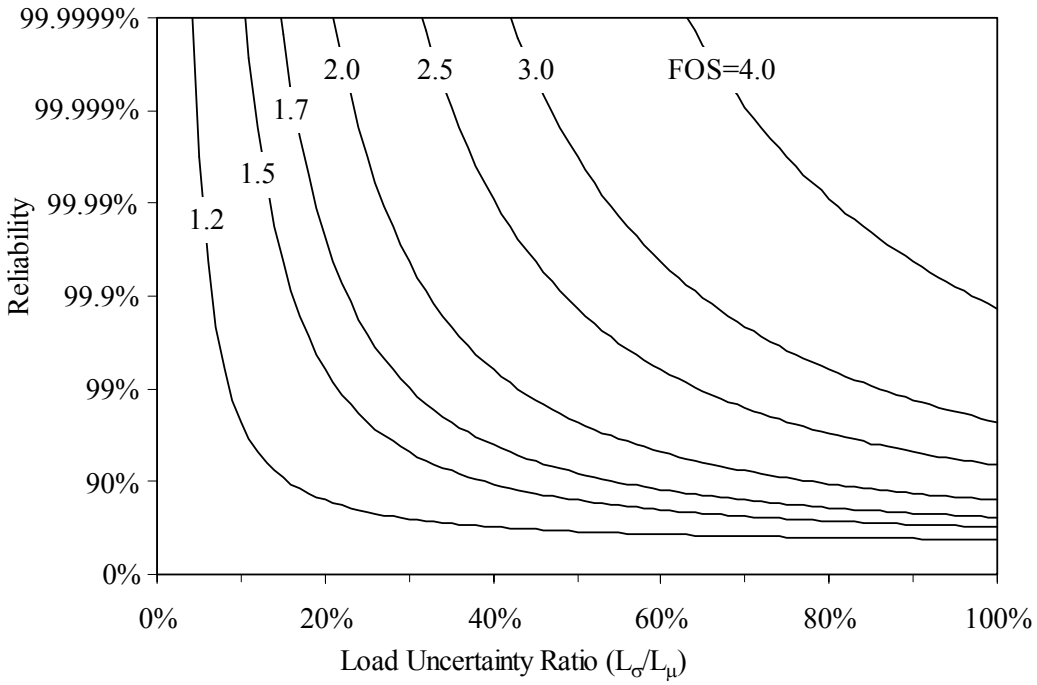

Figure 10a: Example of the strength-load interference method with S_σ/S_μ=0%.

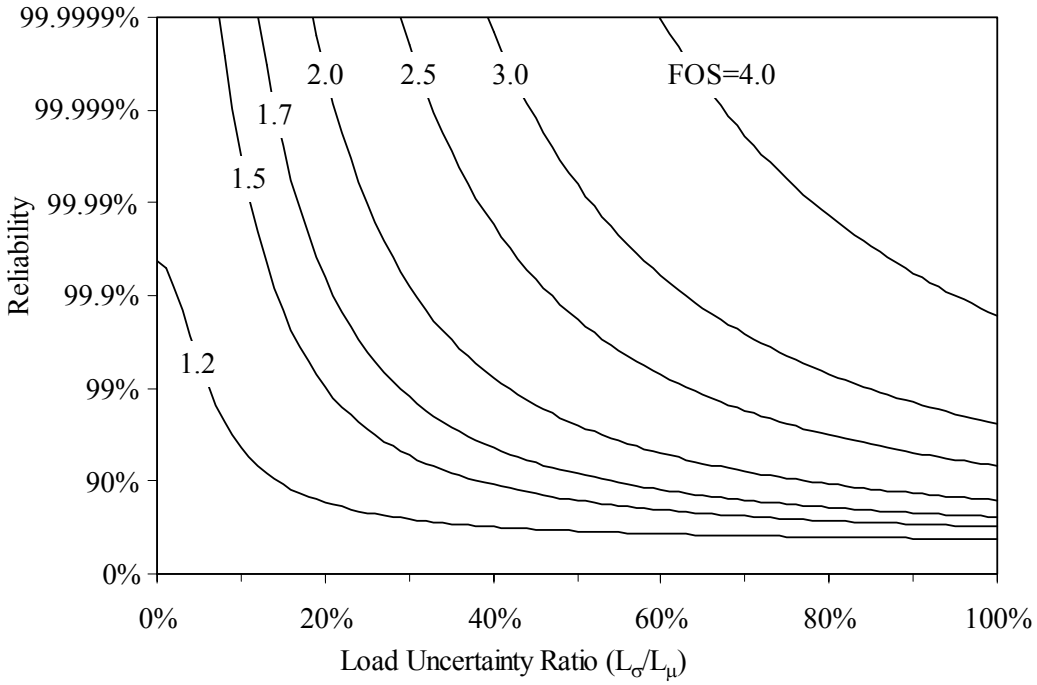

Figure 10b: Example of the strength-load interference method with S_σ/S_μ=5%.

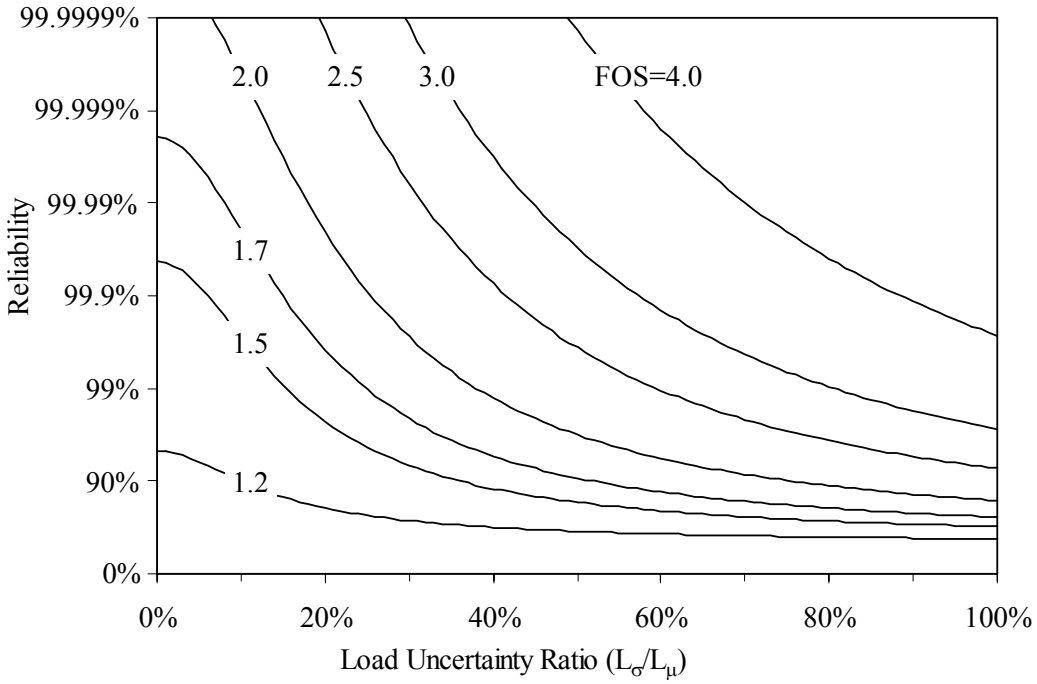

Figure 10c: Example of the strength-load interference method with S_σ/S_μ=10%.

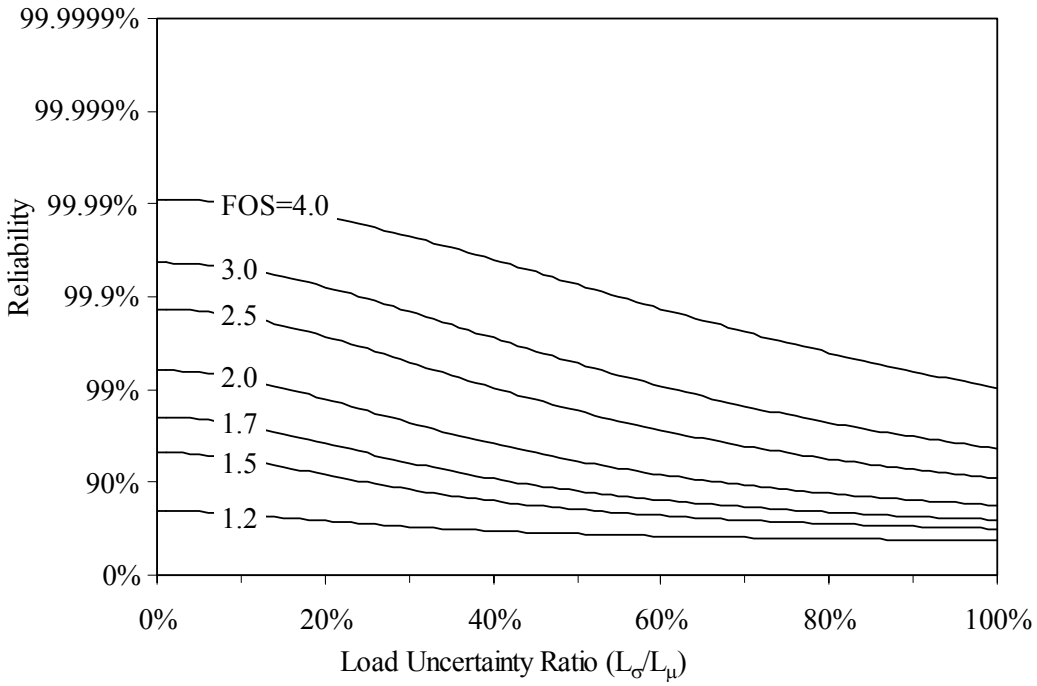

Figure 10d: Example of the strength-load interference method with S_σ/S_μ=20%.

Thermal Reliability Example

With appropriate definitions of thermal strength and load, the interference method can be used to estimate thermal reliabilities of TPS designs. The applied thermal load is the total heat load experienced by the TPS design during planetary entry, and depends on:

1. Trajectory variations,
2. Atmospheric variations,
3. Turbulent transition,
4. Vehicle location and orientation, etc.

The limit thermal load or strength is the total heat load capability of the TPS design, and depends on:

1. Initial temperature,
2. Material properties,
3. Thickness,
4. Attachment to structure, gaps, seals, joints, etc.

In many vehicle designs the TPS thickness is proportional to the total heat load, and thickness may be used to represent thermal load and strength. The minimum TPS thickness that protects the structure from exceeding a design temperature limit is commonly called the "zero-margin thickness". A higher thermal load would require a thicker carbon phenolic, while a lower thermal load would require less material.

For example, a thermal reliability analysis of the carbon phenolic TPS design is possible by assuming that variations in the eight parameters of Table 4 contribute only to the strength uncertainty ratio (S_σ / S_μ), and that no variation occurs in the aerothermal load ($L_\sigma / L_\mu = 0$). The 1σ deviations ($\Delta_{i,1\sigma}$) are one-third of the 3σ deviations ($\Delta_{i,3\sigma}$) in Table 2.

i	Property, P_i	$\partial G/\partial P_i$	$\Delta_{i,1\sigma}$	ΔG_i	$(\Delta G_i)^2$
1	Char Thermal Conductivity (k_c)	+0.995	0.142	+0.141	0.020
2	Virgin Density (ρ_v)	-0.503	0.326	-0.164	0.027
4	Sublimation Activation Temp. (B_s)	-0.292	0.189	-0.055	0.003
5	Virgin Thermal Conductivity (k_v)	+0.210	0.314	+0.066	0.004
6	Blowing Parameter (B^*)	+0.196	0.190	+0.037	0.001
7	Virgin Specific Heat (Cp_v)	-0.172	0.174	-0.030	0.001
8	Char Density (ρ_c)	-0.137	0.102	-0.014	0.000
9	Char Specific Heat (Cp_c)	-0.121	0.274	-0.033	0.001

Table 4: Strength uncertainty ratio for the carbon phenolic design.

For 1σ deviations of these eight parameters the root-sum-square in Eq. (7) gives:

$$S_\sigma = \sqrt{\sum_{i=1}^{n}\left(\left(\frac{\partial G}{\partial P_i}\right)_0 \left(\Delta_{i,1\sigma}\right)\right)^2} = 0.241 \qquad (7)$$

As shown in Table 5, the carbon phenolic thickness that limits the aluminum structure to a maximum temperature of 450°K is equivalent to the mean thermal load and has a non-dimensional thickness of one ($L_\mu = 1$). A TPS design with this thickness ($S_\mu = 1$) has a 50% reliability. Increasing the thermal strength (S_μ), or carbon phenolic thickness, increases IOR and the thermal reliability.

Parameter	Nominal	RSS ($\Delta_{i,1\sigma}$)	RSS ($\Delta_{i,3\sigma}$)	EV
Strength deviation (S_σ)	0.241	0.241	0.241	0.241
Strength mean (S_μ)	1.000	1.241	1.722	2.623
Strength coefficient of variation (S_σ/S_μ)	0.241	0.194	0.140	0.092
Load deviation (L_σ)	0.000	0.000	0.000	0.000
Load mean (L_μ)	1.000	1.000	1.000	1.000
Load coefficient of variation (L_σ/L_μ)	0.000	0.000	0.000	0.000
Factor of safety (FOS)	1.000	1.241	1.722	2.623
Index of reliability (IOR)	0.000	1.000	3.000	6.746
Reliability	0.500	0.841	0.999	1.000

Table 5: The index of reliability increases with carbon phenolic thickness.

Including variation in the thermal load (L_σ), as shown in Table 6, slightly decreases the IOR. In this case, variation in the thermal load is due to only variation in the heat transfer parameter, given by Eq. (8), where as with the parameters in Table 2 for demonstration of the method, $\Delta_{3,1\sigma} = 0.072$ is defined by a random number generator.

$$L_\sigma = \left(\frac{\partial G}{\partial P_3}\right)_0 \left(\Delta_{3,1\sigma}\right) = (0.376)(0.072) = 0.027 \tag{8}$$

Parameter	Nominal	RSS ($\Delta_{i,1\sigma}$)	RSS ($\Delta_{i,3\sigma}$)	EV
Strength deviation (S_σ)	0.241	0.241	0.241	0.241
Strength mean (S_μ)	1.000	1.241	1.722	2.623
Strength coefficient of variation (S_σ/S_μ)	0.241	0.194	0.140	0.092
Load deviation (L_σ)	0.027	0.027	0.027	0.027
Load mean (L_μ)	1.000	1.000	1.000	1.000
Load coefficient of variation (L_σ/L_μ)	0.027	0.027	0.027	0.027
Factor of safety (FOS)	1.000	1.241	1.722	2.623
Index of reliability (IOR)	0.000	0.994	2.981	6.704
Reliability	0.500	0.840	0.999	1.000

Table 6: The index of reliability is decreased by L_σ/L_μ (Eq. 6).

NON-DIMENSIONAL LOAD INTERFERENCE METHOD (NDLI)

The Non-Dimensional Load Interference method (NDLI) was developed to extend the strength-load interference method to thermal design.[6] In this method, three definitions of thermal load and strength were developed to provide TPS designers with several convenient approaches. The total heat load (Q) definition in Eq. (9) is the most general and fundamental, but it does not easily relate to the practical mechanics of a TPS design.

$$FOS = Q_{S,\mu} / Q_{L,\mu} \tag{9}$$

Two more familiar properties of a TPS design, thickness and temperature, correlate to total heat load and may also be used in reliability-based TPS design. The thickness definition in Eq. (10) requires that the TPS thickness vary proportionally with the heat load capability, which generally is true near the zero margin thickness.

$$FOS = G_{S,\mu} / G_{L,\mu} \tag{10}$$

The temperature definition in Eq. (11) requires that the temperature also vary proportionally with the heat load capability.

$$\begin{aligned} FOS &= \left(T_{S,\mu} - T_{r,\mu}\right) / \left(T_{L,\mu} - T_{r,\mu}\right) \\ with\ T_{r,\mu} &= T_{i,\mu} - T_{r,offset} \\ T_{r,offset} &= k_T \left(T_{S,\mu} - T_{i,\mu}\right) \end{aligned} \tag{11}$$

Non-linearities between temperature and heat load are accounted for by selecting an appropriate reference temperature ($T_{r,\mu}$). When the temperature varies approximately linearly with heat load, $T_{r,\mu}$ reduces to simply the mean initial temperature ($T_{i,\mu}$). When the temperature is non-linear with heat load, defining a reference offset temperature, ($T_{r,offset}$) may be necessary, where k_T is a temperature non-linearity factor (see Ref. 6).

Three example applications of NDLI are presented in the following sections. The temperature strength ($T_{S,\mu}$) in these examples is the design temperature limit of the structure, and the temperature load ($T_{L,\mu}$) is the maximum temperature of the structure during the entry trajectory.

Space Shuttle Orbiter Analysis

Reference 7 compares a high fidelity analysis of the thermal response of Reusable Surface Insulation (RSI) tiles at eleven locations to temperatures measured during the second flight of Columbia (OV-102). The analysis and the flight data provide an opportunity to compare the three methods for calculating factors of safety. The NDLI results from Ref. 6 are shown in Fig. 11a-b, where the FOS values for the three different methods are fairly consistent between the heat load, TPS thickness, and measured temperatures, particularly for the windward region.

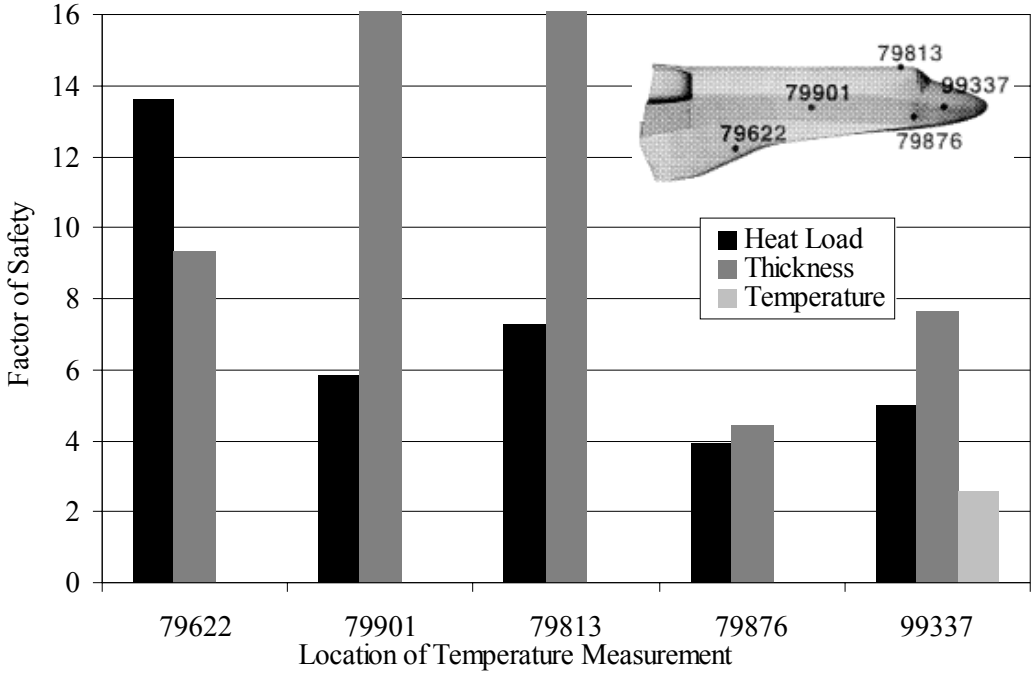

Figure 11a: Factor of Safety (FOS) estimates from heat load, thickness and bond-line temperatures on leeward region (see Ref. 6).

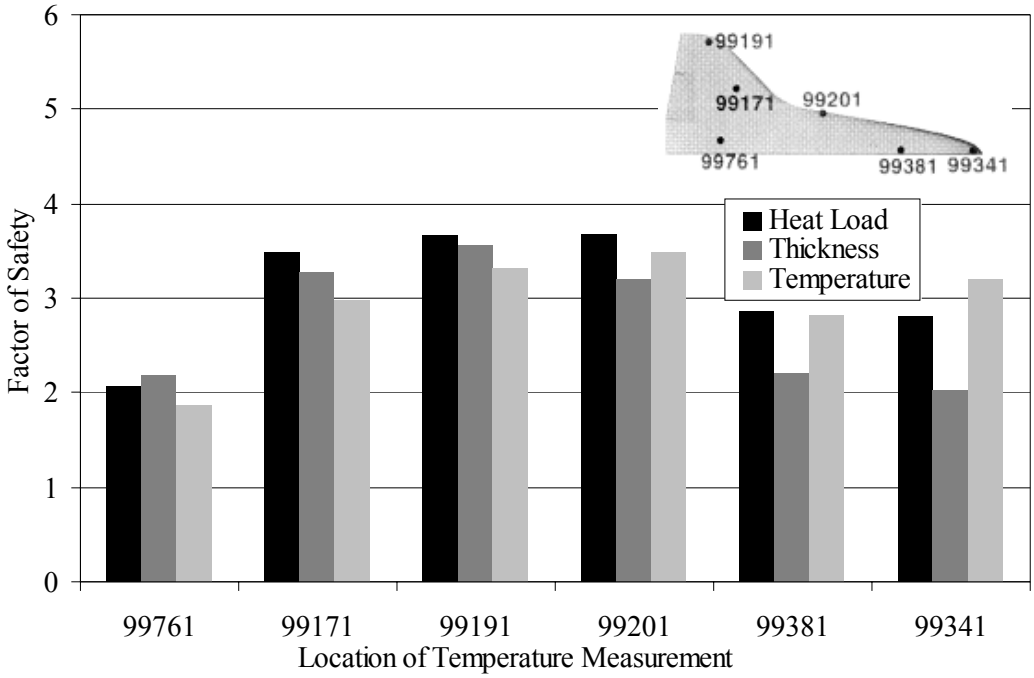

Figure 11b: Factor of Safety (FOS) estimates from heat load, thickness and bond-line temperatures on windward region (see Ref. 6).

Bond-line temperatures were measured by thermocouples located in the adhesive layer attaching the RSI tile to the aluminum structure. Because the adhesive layer is very thin, the bond-line and structure temperatures at the same location are nearly identical. At four

leeward locations there were no temperature data (79622, 79901, 79813, 79876). For the leeward region, some sizable variations in the FOS values are present that may be related to the large uncertainties in the heating, as well as inadequate grid resolution in the numerical analysis. For the windward region, all three methods are more consistent with an approximate mean value near FOS=3. Table 3 indicates that FOS=3 is typically used for less tried or brittle materials under average conditions of loading.

Space Shuttle Orbiter Pre-Flight Assessment

Reference 8 presents an analysis that was done shortly before the first launch of the Space Shuttle Orbiter to establish temperature margins for the RSI tile design at the twelve locations shown in Fig. 12

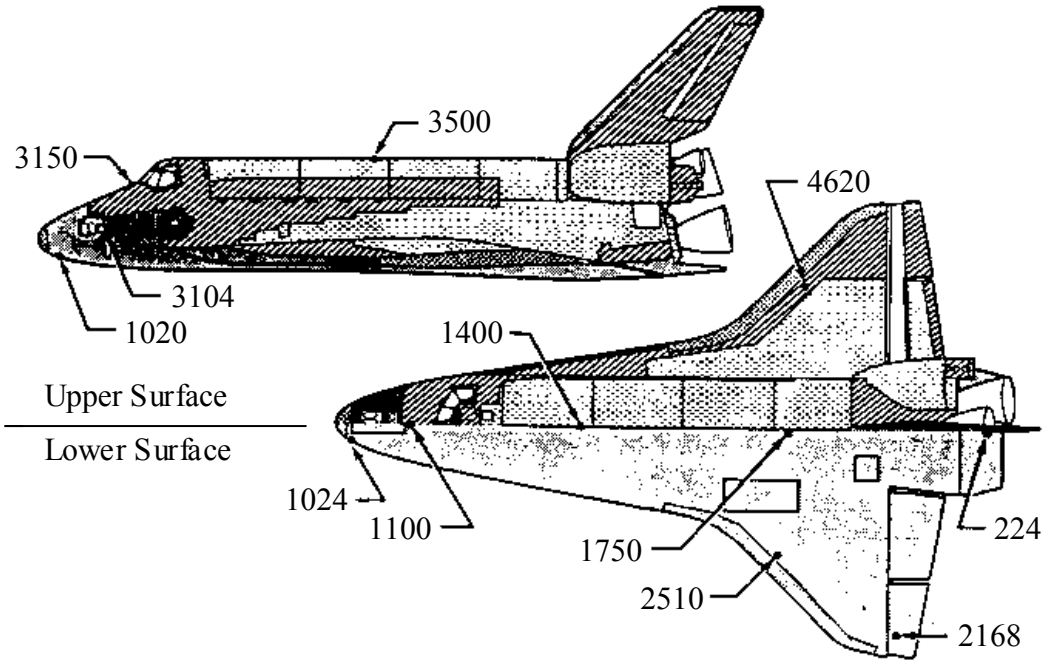

Figure 12: Locations used for analysis in Reference 8.

The RSI tiles are adhesively bonded to an aluminum structure and the temperature margin is equal to the difference between the design temperature limit (450°K) and the maximum temperature of the structure. If uncertainties and variation in both the re-entry heating and the RSI thermal response cause the temperature of the structure to exceed 450°K there is negative margin and the RSI tile has failed to provide adequate protection. The RSS method based on 3σ deviations ($\Delta_{i,3\sigma}$) was used to estimate the margin in Table 8. A negative margin of -19.4°K at location 1100 indicated there was a significant probability that the maximum temperature of the structure would exceed 450°K. Reference 9 applied NDLI to calculate the RSI thermal reliability at the twelve locations in Table 8, and except for location 1100, all of the IOR values were significantly greater than the requirement in Ref. 8 (IOR > 3). The thermal reliability was greater than six nines (0.999 999) at the locations with IOR > 4.768.

Location	L_μ	L_σ/L_μ	S_μ	S_σ/S_μ	Margin*	MOS	FOS	IOR	FOS**
	(°K)		(°K)		(°K)	(°K)			
1020	119.4	0.062	166.9	0.019	23.3	47.5	1.40	5.9	1.32
1024	137.2	0.054	166.9	0.019	5.6	29.7	1.22	3.7	1.28
1100	158.9	0.053	166.9	0.019	-19.4	8.0	1.05	0.9	1.28
1400	86.1	0.069	166.9	0.019	60.6	80.8	1.94	12.0	1.35
1750	72.2	0.101	166.9	0.019	70.6	94.7	2.31	11.9	1.50
3104	90.0	0.124	166.9	0.019	41.7	76.9	1.85	6.6	1.61
3150	44.4	0.223	166.9	0.019	91.1	122.5	3.76	11.8	2.08
3500	69.4	0.161	166.9	0.019	62.2	97.5	2.40	8.4	1.78
4620	61.1	0.183	166.9	0.019	70.6	105.8	2.73	9.1	1.89
2168	55.6	0.214	166.9	0.019	74.4	111.3	3.00	9.0	2.04
2510	119.4	0.088	166.9	0.019	15.0	47.5	1.40	4.3	1.44
224	63.3	0.153	166.9	0.019	72.8	103.6	2.64	10.2	1.75

*Reference 8, **Factor of safety required for a reliability of 0.999 999 (IOR=4.768).

Table 8: Index of reliability from NDLI analysis in Ref. 9.

Overly conservative TPS designs, where the structure is well protected and experiences only very small increases in temperature, are not desirable because the excess TPS mass directly subtracts from the payload capability. For example, three locations in Table 8 (1400, 1750, 3150) are very conservatively designed with IOR ~ 12. One simple approach to optimizing the TPS design at these locations, and moreover for all of the locations in Table 8, uses Eq. (5) with a constant IOR to estimate a new FOS for each location. The last column in Table 8 lists the FOS values for IOR = 4.768, and indicates that it is possible to slightly decrease the RSI thickness at location 1400, such that FOS decreases from 1.94 to 1.35, and yet high thermal reliability (0.999 999) is still provided. On the other hand, slightly increasing the RSI thickness at location 1100, such that FOS increases from 1.05 to 1.28, significantly increases the thermal reliability. Further analysis is required to understand this new approach and develop the appropriate reliability requirements.

Space Shuttle Orbiter Flight Data

In support of the Space Shuttle Orbiter post-flight inspection, structure temperatures are recorded at selected locations on the windward, leeward, starboard and port surfaces. Statistical analysis of this flight data and NDLI were used in Ref. 9 to estimate the thermal reliability at the locations in Fig. 13 where RSI tiles are installed. For consistency with Ref. 8, failure was defined to occur when the structure temperature exceeds the design temperature limit (450°K). Table 9 lists values of the NDLI parameters that were calculated from the temperatures measured on OV-102. The lowest values of IOR occurred at locations on the starboard and port Orbital Maneuvering System pods (S6,P5). At most of the other locations the RSI thermal reliability is significantly greater than 0.999999 (IOR > 4.768) for the missions studied.

Location	L_σ/L_μ	S_σ/S_μ	FOS	IOR
Windward				
B1	0.042	0.034	1.99	12.6
B2	NA	NA	NA	NA
B3	NA	NA	NA	NA
B4	0.060	0.034	2.73	15.8
B5	0.106	0.028	2.06	8.8
B6	0.066	0.040	2.81	13.9
B7	0.095	0.027	1.87	8.2
B8	0.093	0.033	2.10	9.5
B9	NA	NA	NA	NA
B10	0.057	0.036	2.04	11.2
B11	0.102	0.030	3.25	15.9
Leeward				
T1	0.063	0.029	5.46	26.3
T2	0.140	0.026	5.17	21.4
T3	0.084	0.030	3.81	19.6
T4	0.143	0.027	4.26	17.8
T5	0.134	0.027	4.45	19.2
T6	0.111	0.029	3.95	18.4
T7	0.161	0.031	5.20	18.4
T8	0.080	0.015	10.04	52.1
Starboard				
S1	0.059	0.055	2.71	10.6
S2	NA	NA	NA	NA
S3	0.113	0.028	3.76	17.9
S4	0.137	0.062	5.26	12.0
S5	0.106	0.039	4.64	17.3
S6	0.862	0.064	2.67	1.9
Port				
P1	0.053	0.053	2.66	11.1
P2	0.045	0.050	3.19	13.1
P3	0.397	0.053	2.90	4.5
P4	0.080	0.036	4.95	20.1
P5	0.781	0.037	2.51	1.9
P6	0.136	0.043	5.00	15.7
P7	NA	NA	NA	NA
P8	NA	NA	NA	NA

NA – Not Available

Table 9: Non-dimensional parameters calculated from OV-102 structure temperature measurements (Ref. 9).

Table 10 lists the minimum, maximum, and mean values for the four surfaces on two Orbiter vehicles (OV-102, OV-105). In general, S_σ/S_μ is less than L_σ/L_μ indicating that the variation and uncertainty in thermal strength is less than the variation and uncertainty in thermal load. The smallest FOS values occurred on the windward surface and the largest FOS values

occurred on the leeward surface. Mean values of FOS on the windward surfaces of OV-102 and OV-105 were almost identical.

Location	Parameter	OV	L_σ/L_μ	S_σ/S_μ	FOS	IOR
Windward	Minimum	102	0.042	0.027	1.87	8.2
		105	0.050	0.028	1.93	7.7
	Maximum	102	0.106	0.040	3.25	15.9
		105	0.095	0.058	2.77	13.7
	Mean	102	0.078	0.033	2.36	12.0
		105	0.074	0.041	2.35	10.9
Leeward	Minimum	102	0.063	0.015	3.81	17.8
		105	0.140	0.028	3.99	10.3
	Maximum	102	0.161	0.031	10.04	52.1
		105	0.340	0.051	5.79	19.3
	Mean	102	0.114	0.027	5.29	24.1
		105	0.218	0.040	4.83	13.4
Starboard	Minimum	102	0.059	0.028	2.67	1.9
		105	0.051	0.027	2.82	10.6
	Maximum	102	0.862	0.064	5.26	17.9
		105	0.464	0.064	7.40	24.2
	Mean	102	0.255	0.050	3.81	11.9
		105	0.205	0.042	4.80	14.4
Port	Minimum	102	0.045	0.036	2.51	1.9
		105	0.043	0.015	2.96	11.1
	Maximum	102	0.781	0.053	5.00	20.1
		105	0.471	0.039	7.27	48.2
	Mean	102	0.249	0.045	3.53	11.1
		105	0.191	0.029	5.18	20.4

Table 10: Comparison between NDLI parameters for OV-102 and OV-105 (Ref. 9).

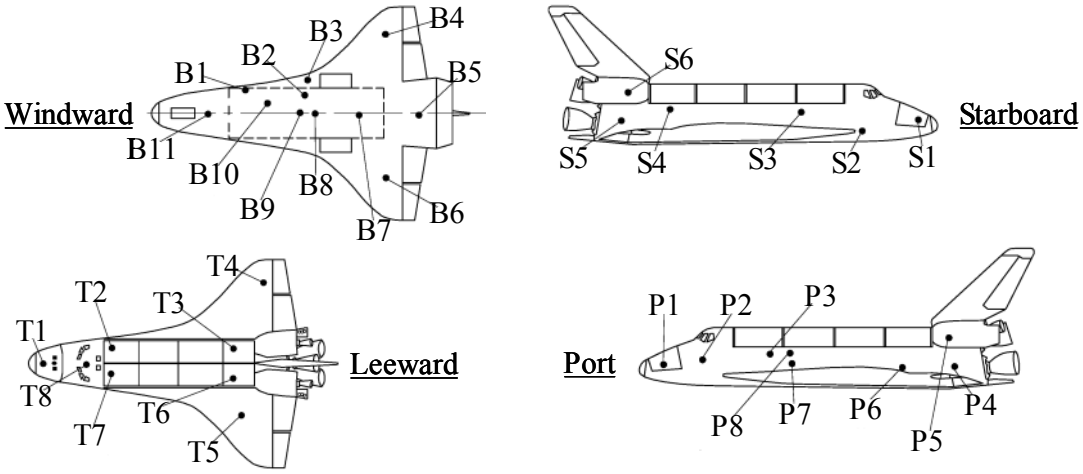

Figure 13: Locations used for analysis in Reference 9.

OV-105 was assembled after OV-102 and incorporated more than ten years of operational experience, modifications and improvements. The FOS and IOR for the port surface on OV-102 and OV-105 are shown in Fig. 14. The original RSI design on the OV-102 Orbital Maneuvering System pods at position P5 had a low index of reliability (IOR = 1.9), which was significantly improved on OV-105 (IOR = 12.6).

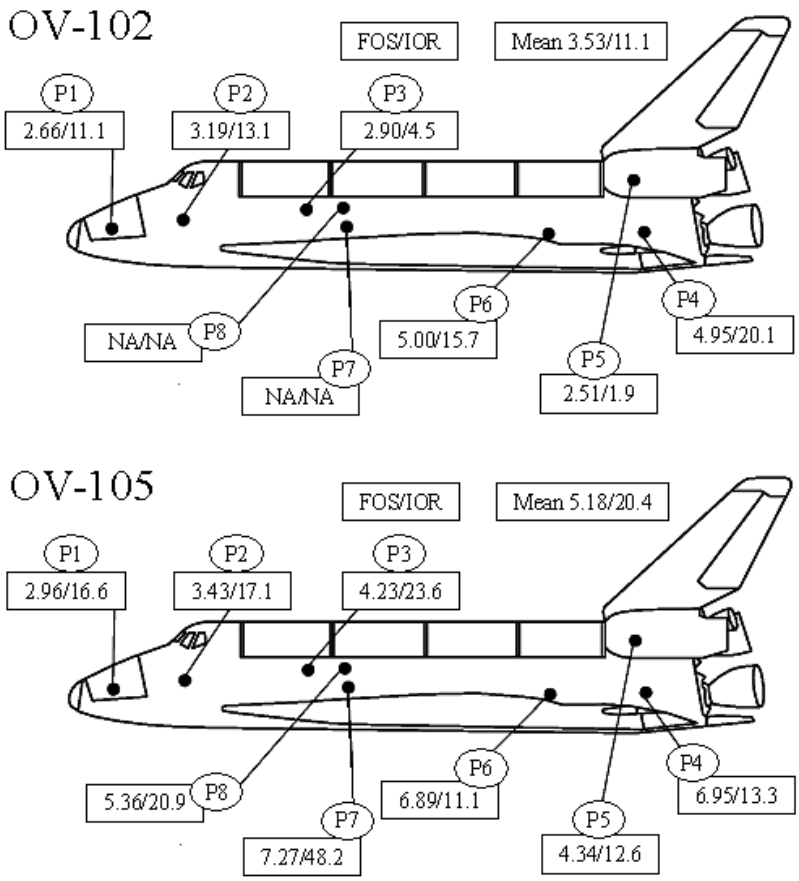

Figure 14: Factor of safety (FOS) and index of reliability (IOR) for the port surface on OV-102 and OV-105 (see Ref. 9).

CONCLUSION

There have been many successful strategies and approaches used in designing TPS components for the severe aerothermal environment experienced during planetary entry. Because of the uncertainties and variations in the entry environment and the resulting thermal response of the TPS material, it is common practice to provide a margin of safety by increasing the TPS thickness. It is important to use standardized quantitative methods in specifying the appropriate margin because the addition of TPS mass reduces the mass available for payload. Reliability based design methods that have been used in the design of mechanical components for nearly 50 years provide valuable experience in developing similar methods for TPS component design.

Sensitivity analysis, by perturbing one parameter at a time in a numerical simulation, provides important insight into the TPS design. An existing sensitivity analysis of carbon phenolic

indicated that eight out of thirty-nine parameters have a large effect on thickness. With the first derivatives from the sensitivity analysis, the extreme value and root-sum-square methods were used to calculate the additional thickness required to compensate for variability in these eight parameters. A comparison of the two methods demonstrated that the extreme value method is more conservative. These methods may be included in a modern integrated design tool and efficiently applied to many locations on a vehicle.

The strength of a design and the load environment are typically not just a single value but have a distribution of expected values. The strength-load interference method calculates reliability from interference of the strength and load probability distributions. By defining the thermal strength and thermal load appropriately the Non-Dimensional Load Interference method (NDLI) applies the strength-load interference approach to TPS design, and calculates thermal reliability from integrated total head load, TPS thickness, or internal temperatures. This flexibility provides TPS designers with a capability to estimate thermal reliability from analysis and experimental measurements.

Acknowledgements

The author gratefully acknowledges that he owes much of his understanding of TPS to the research and educational efforts of his colleagues in the Space Technology Division at the NASA Ames Research Center, and acknowledges their comments, assistance and contributions.

References

[1] Stewart, J. D. and Greenshields, D.H., "Entry Vehicles for Space Programs", Journal of Spacecraft and Rockets, Vol. 6, No. 10, Oct. 1969, pp. 1089-1113.

[2] Kordes, E.E. and Reed R.D., "Structural Heating Experiences On The X-15 Airplane," NASA TMX-711, March 1962.

[3] Heldenfels, R.R., "Structures for Manned Entry Vehicles",, Aerodynamically Heated Structures, edited by Peter E. Glaser, Prentice-Hall, Inc., Englewood Clifs, NJ, 1962, pp.197-218.

[4] Hillberg, L.H., "Influence of Material Properties on Re-Entry Vehicle Heat Shield Design," AIAA/ASME 8th Structures, Structural Dynamics and Materials Conference, March 29-31, 1967, pp.278-288.

[5] Ayyub, B.M. and McCuen, R.H., "Probability, Statistics, and Reliability for Engineers," CRC Press, 1997.

[6] Rasky, D.J. Kolodziej, P., Newfield, M.E., Laub, B., and Chen, Y.K., "Assessing Factors of Safety, Margins of Safety, and Reliability of Thermal Protection Systems," AIAA-2003-4043, June, 2003.

[7] Olynick, D. and Tam, T., "Trajectory-Based Validation of the Shuttle Heating Environment", J of Spacecraft and Rockets, Vol. 34, No. 2, March-April, 1997.

[8] Goodrich, W.D., Derry, S.M., Maria, R.J., "Effects Of Aerodynamic Heating And TPS Thermal Performance Uncertainties On The Shuttle Orbiter," AIAA Paper 79-1042, AIAA 14th Thermophysics Conference, Orlando, FL, June 4-6, 1979.

[9] Kolodziej, P. and Rasky, D.J., "Estimates of the Orbiter RSI Thermal Protection System Thermal Reliability", AIAA 2003-3766, June, 2003.

Nomenclature

A	Reaction constant
B	Reaction constant
B^*	Blowing parameter, $\dot{m} / \rho_e u_e H$
Bs	Activation temperature
EV	Extreme value method
FOS	Factor of safety
Cp	Specific heat
F	Probability of failure
G	Gage or thickness of carbon phenolic
H	Heat transfer coefficient
H_c	Heat of combustion
H_D	Heat of decomposition
H_s	Heat of sublimation
IOR	Index of reliability
k	Thermal conductivity
k_T	Temperature non-linearity factor
L	Load
L/D	Hypersonic lift-to-drag ratio
$\dot{m}$	Mass flux
MOS	Margin of safety
NDLI	Non-dimensional load interference
n	Reaction constant
OV	Orbiter Vehicle
PDF	Probability density function
P_i	Parameter in sensitivity analysis
Q	Heat load
R	Reliability = (1-F)
RSI	Reusable Surface Insulation
RSS	Root-sum-square method
S	Strength
S_w	Wetted surface area
T	Temperature
TPS	Thermal protection system
u	Velocity parallel to surface
V	Volume
x	Integration variable in Eq.(4)
ΔG_E	Thickness increase in Eq.(2)
ΔG_R	Thickness increase in Eq.(3)
ε	Emissivity
η	Transpiration factor
μ	Mean value
ρ	Density
σ	Standard deviation

Subscripts

c	Char or combustion
e	Boundary layer edge
g	Gas
i	Initial
L	Load
r	Reference value
r,offset	Reference offset temperature
S	Strength
s	Sublimation
v	Virgin plastic
μ	Mean value
σ	Standard deviation
0	Nominal or reference values and conditions

Superscripts

1,2	Reaction number